

Feature Article:

Opportunities and Challenges of Quantum Radar

Marco Lanzagorta¹, Jeffrey Uhlmann²

¹U.S. Naval Research Laboratory

²University of Missouri - Columbia

It has been recognized for over half a century that quantum mechanics defines the ultimate limits for sensing devices, and products of that recognition are now on the horizon of practical implementation. One of the most promising of those products is quantum radar, which offers a capability to significantly improve the tradeoff between energy and detection sensitivity compared to classical alternatives. We provide a back-of-the-envelope and implementation-agnostic analysis to glimpse the kinds of expected improvement that a quantum radar could provide for applications of interest. Our analysis relies on relatively simplistic models that are only intended to facilitate an intuitive grasp of quantum-vs-classical distinctions. Such analyses of course cannot lead to definitive conclusions, but we believe they provide evidence that in some contexts quantum radar can be expected to offer realizable practical advantages over classical alternatives. We conclude with a discussion of theoretical and practical obstacles and a high-level summary of what can be said about the present status of quantum radar.

Keywords: Quantum Information, Quantum Sensing, Quantum Radar, Electronic Warfare, Radar Countermeasures.

I. INTRODUCTION

The broad area of study referred to as *Quantum Information Science* (QIS) is concerned with the generalization of classical technologies to obtain improved versions that exploit the larger class of physical properties that can be modeled by quantum physics. In the case of computation this involves the generalization of physical devices capable of representing and manipulating binary states (0 or 1) to obtain devices capable of representing and manipulating a more general class of states that can only be understood using the equations of quantum phenomena. The topic of this paper, *Quantum Radar*, is analogous in that the goal is to generalize the states that are observable using classical radar methods so that the equations of quantum physics can be applied to increase the amount of available information per unit of expended illumination energy.

The objective of this paper is to describe at a high level the fundamental elements of quantum radar and provide insights about why it has the potential to outperform classical radar. Our goal here is *not* to establish definitive statements regarding what may or may not be practically realizable in a given timeframe but rather to provide a level of analysis sufficient to appreciate why quantum radar is of interest and why there is room for debate about its near-term prospects for practical applications. More specifically, our analysis relies on relatively simplistic models that are only intended to facilitate an intuitive grasp of quantum-vs-classical distinctions. In this regard our analyses should be interpreted as offering only back-of-the-envelope evidence that quantum radar is worthy of practical consideration.

The structure of the paper is as follows: We begin with a brief introduction to quantum correlations and the extra information they potentially offer. We then provide a general overview of how a quantum radar can exploit this extra information. This is followed by high-level analyses of the potential advantage of quantum radar over classical alternatives in a set of practical scenarios. We conclude with a discussion of the theoretical and practical issues that must be addressed in order to satisfy the assumptions that underpin the tentative conclusions of our analysis.

II. QUANTUM CORRELATIONS

The most important quantum phenomenon exploited by a quantum radar is quantum entanglement. Let us assume that we have two non-interacting particles A and B separated by an arbitrarily long distance. In the classical world, the measurement of the state of A will not affect the state of B . That is, the measurement of the state of B is independent of the measurement of the state of A . On the other hand, in the quantum world, the measurement of the state of A could affect the state of B . In contrast to the classical world, the measurement of the state of B could depend on the measurement of the state of A . When this happens, it is said that A and B are entangled, and this is a purely quantum property.

A more formal understanding of quantum correlations without discussing quantum dynamics can be offered by introducing the concept of mutual information. Information theory defines the mutual information $I(A : B)$ of two variables A and B as the amount of information obtained about A through the measurement of B [60]. Let us first consider a perfect classical correlation between two binary random variables x and y . Such a correlation can be expressed as:

$$p(x, y) = p_x \delta_{xy} = \frac{1}{2} \delta_{00} + \frac{1}{2} \delta_{11} \quad (1)$$

where δ_{ab} is the Kronecker delta function. In this case it can be shown that the mutual information is given by $I_c(x : y) = 1$. Thus, a perfect classical correlation has a mutual information equal to 1.

On the other hand, a perfect quantum correlation is expressed by a perfectly entangled quantum state denoted by

$$|\psi_{xy}\rangle = \frac{|\psi_{00}\rangle + |\psi_{11}\rangle}{\sqrt{2}} \quad (2)$$

and it can be shown that the mutual information is given by $I_q(x : y) = 2$. That is, perfect quantum correlations have twice as much mutual information as perfect classical

correlations. Increased mutual information between entangled particles immediately suggests improved sensing modalities that can exploit this additional information. In the case of quantum radar, this involves the generation of entangled pairs of photons in the microwave regime.

Clearly, entanglement correlations are an important property for quantum sensing in general and for quantum radar in particular. For example, imagine a state of two entangled photons. One of these photons is held while the other is sent to interrogate some region of space. Our measurement device will measure both the signal photon if it is reflected back to the detector from an object in the environment and background noise photons present in the environment. Because the two original photons are in an entangled state, they contain more mutual information and thus can be more effectively distinguished from noise photons received by the detector than is possible with two perfectly correlated classical entities.

Therefore, quantum entanglement provides an additional source of information that is not available to classical radar. Similarly, entanglement can be used to “hide” the signal photons in the environment noise such that entanglement correlations are the key to detecting them. Although it is impossible to predict with certainty the *extent* to which this theoretical advantage can be realized in practice, entanglement-based sensing technologies could lead to practical benefits in the near future. This optimism is buttressed by recent progress in harnessing quantum entanglement for communications [32], [51], metrology [12], [16], [17], electromagnetic sensing [23], [30], clock synchronization [15], magnetometry [46], seismology [41], [42], and gravimetry [34], [45], [58], with investigated applications extending into space [70] and challenging oceanic environment [47], [48], [71], [72].

III. A GENERAL OVERVIEW OF QUANTUM RADAR

As should be expected, the potential advantage of quantum radar over classical radar comes from exploiting information available from entangled photons in the microwave regime. In this section we discuss how quantum radar offers a capability to significantly improve the tradeoff between energy and detection sensitivity compared to classical alternatives, and we will avoid equations and concentrate our discussion on concepts for illuminating expected theoretical performance. A more detailed presentation of the equations that govern quantum radar performance are discussed in subsequent sections.

A basic conceptual description of a quantum radar is shown in Figure 1 and is somewhat inspired by the theory of *quantum illumination* [2], [52]. At this point it is important to remark that quantum illumination is a protocol to detect the presence or absence of a target at a very specific position of space. As such, quantum illumination on its own is not a quantum radar. However, some of the upper bounds found in quantum illumination can serve as rough estimates to the bounds of future quantum detection and ranging systems.

The quantum radar process begins with a device that generates a pair of highly correlated entangled photons: an *idler* and a *signal* photon. The idler photon is kept in a quantum memory, i.e., a piece of quantum hardware able to faithfully

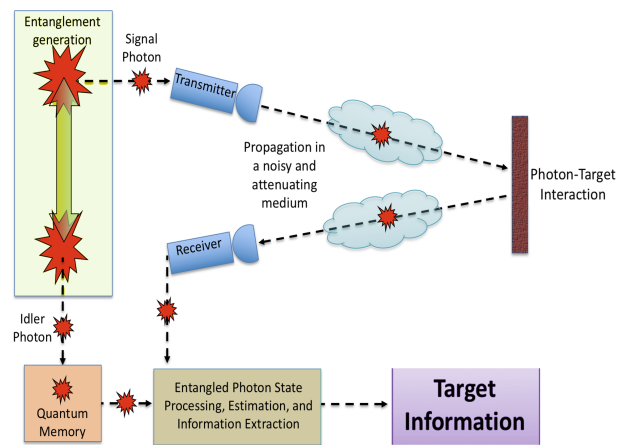


Fig. 1. Conceptual description of an entanglement-based monostatic standoff quantum radar.

hold the quantum state of the idler photon, while the signal photon is transmitted toward some region of space. If a target is present along the transmission path then the signal photon may be reflected back toward the quantum radar. At any given time the quantum radar receiver may measure a reflected signal photon or a noise photon from the environment. Because there is no a priori way to distinguish signal photons from noise photons, each received photon is compared – in a very loose sense that will be made more precise later – to the idler state in the quantum memory. Entanglement correlations eventually allow statistical information from signal photons to be probabilistically distinguished from the noise as the comparison process is integrated over a sequence of many detections.

In the idealized setting each signal photon will either return due to an encounter with a target or will not return and signify the absence of a target along the line-of-sight observation path. In a real-world context some reflected signal photons will not be perfectly-reflected back toward the radar while some that should be perfectly-reflected will be lost due to environmental attenuation, e.g., by being absorbed or scattered/deflected by the intervening atmosphere. Rough back-of-the-envelope calculations suggest that the integration process will require in excess of 10^9 entangled photons to have a probability of detection of 0.8 for a static target (2m diameter flat circular target with 0.1 reflectivity oriented in the specular direction) located 25km away in low visibility atmospheric conditions (300m visibility due to fog or clouds) using a quantum radar operating in the X-band frequency (3.2cm) and a 2m diameter receiver/transmitter. Each set of 10^9 photons is called a quantum radar *signal package*.

An ideal source of entanglement would produce entangled pairs on demand; that is, with near 100% certainty the source produces exactly 1 entangled pair at the push of a button. However, such sources are in their infancy and not commercially available. In optical frequencies, where most work on photon entanglement has been carried out, one can generate entangled pairs via Spontaneous Parametric Downconversion (SPDC) using a pulsed laser through a non-linear crystal [31]. Pulsing

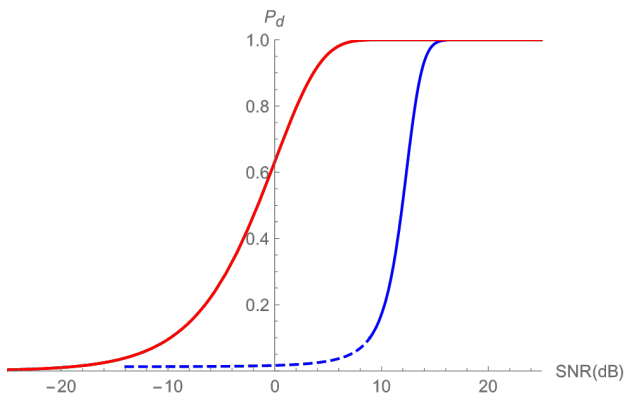


Fig. 2. Theoretical P_d vs. SNR for entangled quantum radar (red) and classical radar (blue).

the laser allows one to timestamp the event; however, each pulse has a very low probability of containing a photon pair [26]. Even with this limitation, using a PPKTP crystal and a 2 ps pulsed laser, it is possible to generate 10^5 entangled pairs per second for each milliwatt of pump power [27], [28]. For a conservative model using off-the-shelf technology, we can assume a pump power of 100mW, and we will therefore have the capability to generate 10^7 entangled pairs per second. Each of these photons is temporally separated and their integration can be carried out with standard equipment.

In the microwave regime the situation is far less advanced, with the study of how to generate entangled microwave photons only receiving significant attention in the last few years. In addition, microwave frequencies impose a limit on the number of distinguishable/independent optical modes available [19]. Indeed, the number of distinguishable modes (M) available for a single illuminator-detector is $M = W \times T$, where W is the bandwidth and T the period of the signal. Assuming that a quantum sensor operates in the X-band at 10 GHz, and works with a 40% fractional bandwidth, then the bandwidth is approximately 4 GHz. If the signal pulses are emitted with a period of $1 \mu\text{s}$ then $M \approx 4 \times 10^3$, i.e., much less than the $M \approx 10^9$ required in the previous example. In general, the number of distinguishable modes available in the primary radio-spectrum bands is impractically small. To overcome the constraints imposed by small M , it has been proposed a distributed architecture of quantum sensors for which the effective size of M can be increased [33], [35]. A different approach to this problem is the use of multiple-input multiple-output channels using beam-splitters [25].

In order to determine the expected performance of a quantum radar, we use theoretical models that will be described in more detail in subsequent sections [40]. According to these models, the advantage of quantum radar (red) as compared to classical radar (blue) is shown in Figure 2 in terms of the detection probability (P_d) vs. the signal-to-noise ratio (SNR) in decibels. In the quantum case the theoretical SNR is computed using signal packages, not individual photons. The detection probability curve for classical radar has been empirically well-characterized in the form of Albersheim's formula [67], [68], while the detection probability for quantum radar has been

derived using standard methods from quantum detection and estimation theory [22]. We notice that the quantum expression for the detection probability has been experimentally validated in the optical and microwave regimes [54]. These expressions are expected to remain valid for a wide range of frequencies because the underlying theory of quantum electrodynamics is valid for all frequencies.

Clearly, the attenuating environment; target reflectivity; environmental noise; signal beam divergence; electronic noise; and other sources of noise due to imperfect electronics and optical equipment will reduce the SNR of both systems. To avoid enumerating a comprehensive list of assumptions regarding the operational environment and the quality of available technology, in this section we will only discuss the theoretical performance relative to SNR. That is, the notion of SNR in Figure 2 is taken to encapsulate all possible sources of noise, including atmospheric attenuation, target reflectivity, and target cross section. Thus, the comparison offered by this figure is valid as long as both systems exhibit the exact same SNR.

Examining the curves in Figure 2 we can observe that in the extremely high SNR regime (above 15dB) the detection probability of the two sensors is about the same and very close to 1 (i.e., we can determine almost perfectly the presence of a target). In the extremely low SNR regime (below -15dB), the detection probability of both sensors is also about the same but very close to 0 (i.e., we have the same probability of determining the presence of the target as if we used a coin flip). In both extreme situations quantum radar does not offer any advantage over classical radar.

It is in the low SNR, at around 3dB, where quantum radar can be seen to provide a higher detection probability than classical radar. At 0dB, for instance, quantum radar can provide a significant detection probability (P_d about 0.65) while the detection probability using classical radar is practically zero (though we could always increase the power of the classical radar signal to achieve a higher detection probability). Thus, the real advantage of quantum radar is simply being able to detect the presence of a target using less transmitted energy, i.e., with a smaller number of photons.

The advantage of quantum radar in the low SNR regime (-5dB to 10dB) appears to be a fundamental property of these systems. For example, recent theoretical studies on synthetic aperture quantum radar and quantum radar Doppler filters to reduce the effects of clutter consistently predict a quantum advantage strictly limited to the low SNR regime [49], [50].

It must be emphasized that these comparisons are only valid when both systems exhibit the exact same SNR. Thus, no further assertions can be made about the relative performance of classical and quantum radar systems simply based on Figure 2. For example, a classical radar implemented with low-noise electronics could have an SNR of 10dB when observing a target 1km while a quantum radar built with noisy electronics could have the same SNR only for a target 10m away. After a careful link budget analysis, however, quantum radar appears to emerge as an intriguing theoretical concept with potentially important practical applications. For example, under certain conditions quantum radar could help to determine with high probability the presence of an adversary while maintaining

a low probability that the sensing will be detected by that adversary. Lower power requirements are also desirable for space-borne applications where power consumption is a highly important consideration [70]. Furthermore, the underlying physical principles of quantum radar could also be used to design low-brightness medical imaging devices to minimize patient exposure to the probing radiation.

Although the previous analysis has been entirely theoretical, recent research suggests that robust quantum radar systems are potentially viable [14], [55], [64], [65]. For example, recent theoretical and experimental results indicate that it is possible to generate, entangle, detect, perform interferometry, and conduct signal processing and sensing using a large number of entangled photons in the optical and microwave wavelengths [2], [13], [62], [73]. Actually, some quantum illumination experiments with optical and microwave wavelengths have already been successfully carried out and they have demonstrated improved performance over classical detection methods [3], [64].

Therefore, there does not appear to be any fundamental obstacle to the physical realization of a quantum radar. As will be discussed in the next section, however, there are many important challenges that remain to be solved and are crucial for the successful development of quantum radar.

IV. QUANTUM HYPOTHESIS DISCRIMINATION

In this section we will briefly describe how certain entangled photon states can be characterized by covariance matrices and how they are used for target detection.

A. Covariance Matrix of Photon States

Consider a Gaussian entangled state as the one produced in spontaneous parametric down-conversion (SPDC)¹ and let $|\Psi_{si}\rangle$ denote the state of a system made of a zero-mean Gaussian package of signal (s) and idler (i) photon states. Formally, in an occupation number Fock space, this state is given by:

$$|\Psi\rangle_{si} = \sum_{n=0}^{\infty} \sqrt{\frac{N_s^n}{(N_s + 1)^{n+1}}} |n\rangle_s |n\rangle_i \quad (3)$$

where N_s is the average photon number, and $|n\rangle_s$ and $|n\rangle_i$ denote the photon state of n signal and n idler photons respectively [31], where the subindices i and s refer to the idler and signal photons, respectively.

We can define a parameter λ as:

$$\lambda \equiv \sqrt{\frac{N_s}{N_s + 1}} \quad (4)$$

which can be used to parametrize a series expansion of the Gaussian state. Thus, if $\lambda \ll 1$, then:

$$|\Psi\rangle_{si} \approx \sqrt{1 - \lambda^2} |00\rangle + \lambda |11\rangle \quad (5)$$

This equation represents a quantum state made of 0 idler and 0 signal photon states with probability $\approx 1 - \lambda^2$, and a state

¹SPDC may not be the best or most optimal way to generate microwave photons. However, we can expect that the outgoing pair of entangled photons will be described by the same type of mathematical expressions.

with 1 idler and 1 signal photon state with probability $\approx \lambda^2$. In practice, $\lambda \approx 10^{-2}$ [31]. And therefore $N_s \approx 10^{-4} \ll 1$. That is, these entangled states are very “diluted states” of signal and idler photons in the sense that their average number is very small.

A general two-mode Gaussian state can be represented through a Wigner-distribution covariance matrix that has the following form:

$$\Gamma_{si} = \frac{1}{4} \begin{pmatrix} S_s & 0 & C_s & 0 \\ 0 & S_s & 0 & C_i \\ C_s & 0 & S_i & 0 \\ 0 & C_i & 0 & S_i \end{pmatrix} \quad (6)$$

given in terms of only four parameters [53]. In a sense, the S_i terms can be understood to be related to the intensity of the idler component, while the S_s are related to the signal photon intensity. On the other hand, the C_i and C_s terms are related to the degree of entanglement or correlation between both components.

Mathematically, quantum entanglement is understood as a characteristic of quantum states over two different variables that cannot be separated as the product of two individual states (one for each variable and independent of the other). Thus, most criteria to measure the degree of entanglement in a quantum system is related to a measure of the separability of the state of the system as the product of the state of the individual components. Following this rationale, it can be shown that the necessary and sufficient condition for entanglement between the signal and idler photons in the Gaussian state can be simply written as:

$$(S_s S_i - C_s^2)(S_s S_i - C_i^2) < (S_s^2 + S_i^2) + 2|C_s C_i| - 1 \quad (7)$$

which is usually referred as *Simon's criteria* [66]. This is the mathematical criterion for two photon Gaussian state to be expressed as the product of two individual and independent photon states.

For simplicity, we can also define:

$$f \equiv (S_s S_i - C_s^2)(S_s S_i - C_i^2) - (S_s^2 + S_i^2) - 2|C_s C_i| + 1 \quad (8)$$

as a measure of entanglement/correlation between the components of the system, and Simon's entanglement criteria reduces to $f < 0$. That is, the Gaussian system is entangled if $f < 0$ and it is not entangled if $f \geq 0$.

For the case under consideration, we have:

$$S \equiv S_i = S_s = 2N_s + 1 \quad (9)$$

and:

$$C_q \equiv C_s = -C_i = 2\sqrt{N_s(N_s + 1)} \quad (10)$$

which satisfies the inequality and therefore, as expected, $|\Psi\rangle_{si}$ is an entangled state. In addition, one can easily find the approximate value of C_q for which the state showcases minimum entanglement. It is found that this bound corresponds to approximately $C_c = 2N_s$. Therefore, if $N_s \gg 1$ then $C_q \approx C_c$ and the entanglement is negligible. On the other hand, if $N_s \ll 1$ then $C_q \gg C_c$ and the state is highly entangled. In other words, low brightness ($N_s \ll 1$) Gaussian states from SPDC showcase strong nonclassical signatures and a high

degree of entanglement [22] while high brightness ($N_s \gg 1$) Gaussian states from SPDC have minimal entanglement.

B. Target Detection

As discussed above, the signal photon state may be bounced back toward the detector and be registered/measured, or the detector may just measure noise photon states. Therefore we have two detection hypotheses:

- Hypothesis H_0 : there is no target within range of the detector. In this case, the detector will only measure noise photon states. In this case the Wigner distribution covariance matrix is given by:

$$\Gamma_{ri}^{(0)} = \frac{1}{4} \begin{pmatrix} B & 0 & 0 & 0 \\ 0 & B & 0 & 0 \\ 0 & 0 & S & 0 \\ 0 & 0 & 0 & S \end{pmatrix} \quad (11)$$

where:

$$B = 2N_b + 1 \quad (12)$$

with N_b representing the average number of noise photons. From this the entanglement criterion function is:

$$f_{ri}^{(0)} = 16N_s N_b (N_s + 1)(N_b + 1) \geq 0 \quad (13)$$

which means that the state is not entangled.

- Hypothesis H_1 : the target is within range but only a portion of the photons κ return to the detector. In this case, the Wigner distribution covariance matrix is given by:

$$\Gamma_{ri}^{(1)} = \frac{1}{4} \begin{pmatrix} A & 0 & C_r & 0 \\ 0 & A & 0 & -C_r \\ C_r & 0 & S & 0 \\ 0 & -C_r & 0 & S \end{pmatrix} \quad (14)$$

where:

$$A = 2(\kappa N_s + N_b) + 1 \quad C_r = 2\sqrt{\kappa N_s (N_s + 1)} \quad (15)$$

and the separability criterion function is given by:

$$f_{ri}^{(1)} = -16N_s (N_s + 1)(\kappa - N_b)(N_b + 1) \quad (16)$$

which means that the state is not entangled if $\kappa \leq N_b$.

In the case of microwaves, the number of noise photons correspond to $N_b \approx 10^4$. Indeed, solar radiation has a strong contribution to noise in the microwave regime. In such a case, $f_{ri}^{(1)}$ is always positive, which means that no entanglement survives the noisy microwave environment produced by solar radiation. Therefore, the states at the detector may *not* be entangled under both hypotheses. Indeed, the environment obliterates any degree of entanglement by the time the signal photon state returns to the detector. Nonetheless, some of the initial quantum correlations expressed in the highly non-classical state with covariance matrix Γ_{si} persist even after total annihilation of the entanglement [22].

The next step is to discriminate between both hypotheses. In theory this could be accomplished by measuring the operator \hat{A} given by:

$$\hat{A} = \hat{\rho}_{ri}^{(1)} - \hat{\rho}_{ri}^{(0)} \quad (17)$$

where $\hat{\rho}_{ri}^{(1)}$ and $\hat{\rho}_{ri}^{(0)}$ are the density matrices that correspond to hypotheses 1 and 0, respectively [20]. These density matrices are related to the covariance matrices $\Gamma_{ri}^{(0)}$ and $\Gamma_{ri}^{(1)}$. If the measurement yields a positive value then the target is declared to be within range. On the other hand, if the measurement yields a negative number, the target is declared to be out of range. Needless to say, it is not a simple task to find the eigenvalues of \hat{A} . As a consequence, as will be shown in the following section, in the most general case our theoretical analysis can only determine upper bounds on the detection error probability.

V. DETECTION ERROR PROBABILITY BOUNDS

The detection error probability ϵ represents the probability that the sensor registers a false detection, i.e., registers a detection when no target is present or fails to register a detection when a target is present. In other words, ϵ reflects the probability that the conclusion implied by a particular sensor observation (*detect* or *no-detect*) is wrong. Alternatively, $(1 - \epsilon)$ represents the probability that the conclusion implied by the observation is correct.

In the limit of a non-informative sensor that returns essentially random results, the probability that the conclusion implied from a particular observation is incorrect is equivalent to a coin toss, i.e., $\epsilon = 0.5$. This is a somewhat counterintuitive measure in the sense that $\epsilon = 0$ and $\epsilon = 1$ represent limits that can only be achieved by a perfect sensor, albeit with the latter case representing a situation in which the labels for *detect* and *no-detect* events have been reversed. We choose this measure because it has mathematically convenient properties and is reasonable as long as it is assumed that ϵ is less than or equal to 0.5, which should be true for any realistic properly-calibrated sensor.

As will be shown later, thermal background noise tends to dominate over shot noise and dark counts in low-SNR scenarios for standoff detection, so to simplify our analysis we will define a high-noise scenario as being in the regime in which the joint impact on SNR of noise sources other than background radiation is negligible.

In the case of Gaussian signal states described in the previous section, the detection error probability can be derived using conventional quantum optical models. We will consider two cases, a “quantum” case in which the signal and idler photons are entangled, and a “coherent” case which does not use entangled photons. In the second case, even though there is no entanglement, we assume that we still have photon-by-photon control. As such, this case can be understood as the best possible sensor that does not use entanglement. While such a coherent sensor may be expensive and unnecessary in practice, it offers a bound to better understand the performance of other sensors that do not use entanglement.

We begin by focusing on the the low-brightness, high-noise, low-reflectivity regime in which:

$$\begin{aligned} N_s &\ll 1 \\ N_b &\gg 1 \\ \kappa &\ll 1 \end{aligned} \quad (18)$$

where as before, N_s is the average photon number per mode, κ represents photon loss from both target absorption and atmospheric attenuation, and N_b gives the average background number of photons. These permit upper bounds to be obtained for the detection error probabilities ϵ_q and ϵ_l for entangled-photon and coherent (non-entangled) sensors, respectively, as

$$\epsilon_q \leq P_q \equiv \frac{e^{-M\kappa N_s/N_b}}{2} \quad (19)$$

and

$$\epsilon_l \leq P_l \equiv \frac{e^{-M\kappa N_s/4N_b}}{2} \quad (20)$$

where M is the number of signal photons emitted to produce a detect or no-detect conclusion [22]. To clarify the notation, the total signal is given by the product $M \times N_s$. For all of our analyses we will fix $N_s = 10^{-4}$ and $N_b = 10^4$, and we will scale the signal only with M .

It can be observed that the difference between both upper bounds is a factor of 4 in the denominator of the exponent, which implies that entanglement-based quantum radar offers a 6 dB advantage in the error-probability exponent over the optimal coherent receiver that does not use entanglement.

It is important to remark that most of the subsequent analysis is entirely based on the detection error probability bounds described by equations (19) and (20). In addition, we clarify that when we compare an entanglement-based quantum radar with a coherent sensor as defined above, we will always assume that both operate with the exact same number of photons M and the same signal photon density N_s . Clearly, it is much simpler to generate a large number of non-entangled photons, but our goal is to compare both systems operating with the same energy.

The upper bounds presented above suggest that the average SNR per signal pulse for both types of sensor can be approximated as:

$$SNR \approx \frac{M\kappa N_s}{N_b} \quad (21)$$

As long as SNR is not large, the upper bounds for ϵ_q and ϵ_l are valid to within a relatively small percentile error and the approximation will tend to capture the dominant effects of noise in the regime of interest (between -25 and 25 dB). Based on this observation, and more importantly because of its mathematical simplicity, we will assume its use throughout the following analyses.

Alternatively, we could define snr as the *signal-to-noise ratio per signal photon* as:

$$snr \approx \frac{\kappa N_s}{N_b} \quad (22)$$

Under our characterization of what constitutes a challenging noisy environment, the average *snr per signal photon* is approximately -90 dB, which includes all environmental sources of attenuation. Thus, to achieve an order-one effective SNR per signal pulse the system will need $M \approx 10^9$ photon states, whether they be entangled in the case of a quantum radar or unentangled in the case of a coherent sensor. In other words, each observation – i.e., total integration of information leading to a detect or no-detect conclusion – requires on the order of

10^9 photons to be emitted, e.g., $\sim 10^9$ Gaussian entangled photon states in the case of a quantum radar.

VI. THEORETICAL COMPARISON

Let us now examine the theoretical performance of three radar types in a challenging regime typical for standoff sensing applications:

- A quantum radar that uses entangled photon states (a signal and an ancilla);
- A coherent radar that uses non-entangled photon states but allows single-photon control; and
- A classical radar system described by Albersheim's formula.

To compare these three sensors we will use detection error probability as our measure of performance. The detection error probability for the first two sensors has already been presented in the previous section, so now we need to obtain an equivalent expression for the classical radar case.

Following our general approach of exploiting simplifying approximations to make the flow of analysis easier to follow, we will use Albersheim's empirically-derived formula to express the approximate average per-pulse SNR for a classical radar when integrated over n independent pulses:

$$SNR_n = \frac{A + 0.12AB + 1.7B}{n} \quad (23)$$

with

$$\begin{aligned} A &= \ln\left(\frac{0.62}{P_{fa}}\right) \\ B &= \ln\left(\frac{P_d}{1 - P_d}\right) \end{aligned} \quad (24)$$

where P_d is the probability of correct detection and P_{fa} is the probability of false alarm [67]. From this the detection error probability bound P_c can be defined to be

$$P_c \equiv \frac{1 - P_d}{2}. \quad (25)$$

The accuracy of Albersheim's approximation is reported ([67], [68]) to be within 2 dB for $0.1 \leq P_d \leq 0.9$ and $10^{-7} \leq P_{fa} \leq 10^{-3}$. Based on these range of values, for subsequent comparison analysis we will favorably assume a conservative value of $P_{fa} = 10^{-7}$ that is optimistic with respect to the true performance of a classical radar system described by the Albersheim's equation.

Figure 3 compares the relative performance of the three sensors based on the theoretical models that determine the upper-bound detection error probability. For the classical case we have extrapolated the line that corresponds to the Albersheim's equation to smaller values of the detection probability ($0.0126 \leq P_d \leq 0.999$).

It can be observed that in the low SNR and low-brightness regime the quantum sensor significantly outperforms the coherent and the classical sensors, and these results are consistent with those previously reported in the literature [22], [37]. This advantage comes from the quantum sensor's ability to extract additional entanglement-derived information from the relatively small fraction of signal photons that are received.

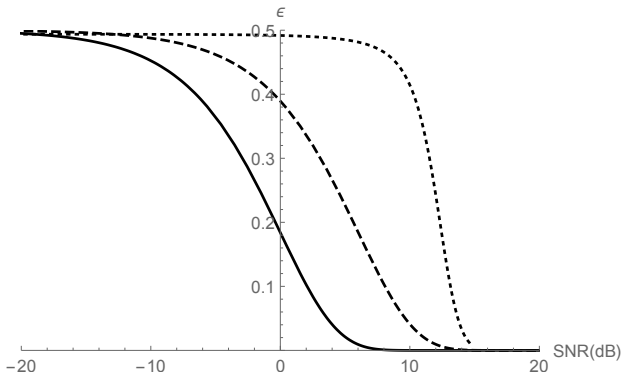


Fig. 3. Theoretical upper bound on the detection error probability ϵ for a quantum radar with $M = 10^9$ entangled photon states (P_q - solid line), a coherent unentangled photon state radar (P_l - dashed line), and a classical radar described by the Albersheim's formula (P_c - dotted line) with respect to SNR in dB.

As the SNR becomes very small the detection error probability of all three sensors rapidly approaches the same non-informative limit of 0.5. As the SNR becomes very large the performance of the three sensors similarly converge but to the idealized limit in which the detect versus no-detect status of each observation is always correctly assigned. It has been argued, however, that in theory the performance of the quantum sensor should dominate between these two limits because its signature will be amplified by additional entanglement-derived information [37], [44], but at present there is no way to determine whether this advantage can actually be realized in practice, i.e., whether entanglement-derived information can exceed the information cost incurred by the practical overhead required to obtain it.

VII. SIZE OF THE QUANTUM PULSE

Figure 4 shows the upper-bound detection error probability ϵ as a function of $\log_{10} M$ (log of the number of signals) for entangled (solid line) and unentangled (dashed line) photon states when the signal-to-noise ratio per photon is $snr = -90$ dB. It can be seen that both sensors converge to the non-informative limit of $\epsilon = 0.5$ as M becomes very small while in the case of very large M the advantage of the quantum sensor is lost because the coherent sensor will tend toward the same maximum information limit due to the plentiful availability of unentangled photons. In other words, there is decreasing benefit gained from additional entanglement-derived information because there is no shortage of classical information available to both sensors from the large number of received photons.

This motivates the determination of the optimal number of signal photons to maximize the potential advantage achievable by a quantum sensor in the high-noise regime under consideration. This is of interest because it can be used to identify a particular context in which a quantum advantage is most likely to be achieved *in practice*. As already mentioned, it is the tradeoff between improved information exploitation and the practical constraints incurred by a more complex system that will determine whether a true quantum advantage can be

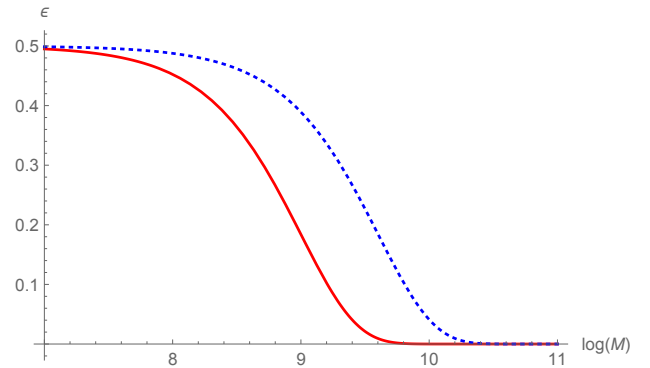


Fig. 4. Upper bound on the detection error probability when the signal-to-noise ratio per photon is $snr = -90$ dB with respect to $\log_{10} M$ for entangled (solid line) and unentangled (dashed line) photon states.

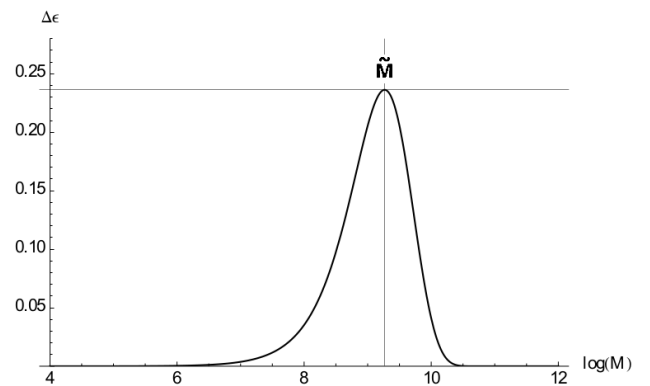


Fig. 5. Difference in the detection error probability upper bounds for the entangled and non-entangled photon states with respect to $\log_{10} M$ when the signal-to-noise ratio per photon is $snr = -90$ dB.

realized. Let $\Delta\epsilon$ be the difference of the detection error upper bounds for the quantum (entangled) and non-quantum sensors:

$$\Delta\epsilon \equiv P_l - P_q. \quad (26)$$

Thus the goal is to determine the value of M that tends to maximize $\Delta\epsilon$.

Figure 5 shows how $\Delta\epsilon$ varies with respect to $\log_{10} M$ (still with an assumed signal-to-noise ratio per photon $snr =$

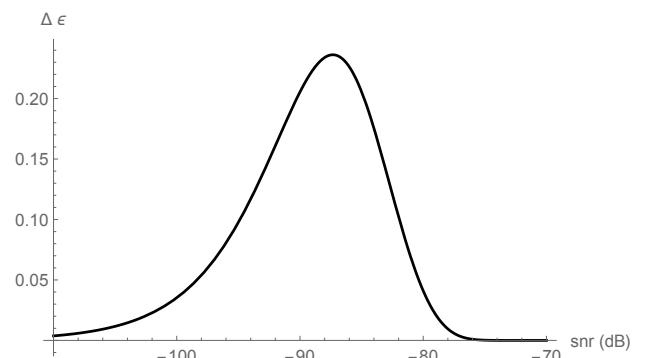


Fig. 6. Difference in the detection error probability upper bounds for the entangled and non-entangled photon states with respect to the signal-to-noise ratio per photon snr in dB when $M = 10^9$.

−90 dB) and there is a single clear and maximizing value. This value, which we will denote as \tilde{M} , can be analytically determined from:

$$\frac{d}{dM} \Delta\epsilon = \frac{1}{2} \left(\alpha e^{-M\alpha} - \frac{\alpha}{4} e^{-M\alpha/4} \right) = 0 \quad (27)$$

to give

$$\tilde{M} = \frac{4 \ln 4}{3 \alpha} \propto \frac{1}{\alpha} \quad (28)$$

where $\alpha \equiv SNR$. With a signal-to-noise ratio per photon of $snr = -90$ dB we obtain $\log_{10} \tilde{M} \approx 9.2668$, which can be seen to be consistent with peak value shown in Figure 5. Notice that at this signal-to-noise ratio per photon and with the optimal number of photons \tilde{M} , we obtain a signal-to-noise ratio per pulse of $SNR \approx 2.668$ dB.

It is important to observe that at this \tilde{M} the desired maximizing value for $\Delta\epsilon$ is:

$$\tilde{\Delta\epsilon} = \frac{3}{8} 4^{-1/3} \approx 0.2362. \quad (29)$$

Again, this is consistent with what is observed in Figure 5 as $P_l(\tilde{M}) \approx 0.3150$ and $P_q(\tilde{M}) \approx 0.0787$. It should be noted that the value of $\tilde{\Delta\epsilon}$ is virtually independent of the signal-to-noise ratio per photon of snr and therefore $\tilde{\Delta\epsilon}$ represents the largest advantage regardless of the level of noise. Figure 6 shows the difference in the upper bound detection error probabilities in the quantum and non-quantum cases. As should be expected, there is an optimal value of the signal-to-noise ratio per photon snr for a given M and $\tilde{\Delta\epsilon}$ bounds the maximum achievable quantum advantage.

VIII. IMPACT OF EARTH ATMOSPHERIC ATTENUATION ON PERFORMANCE

In this section we further narrow the focus of analysis to consider only atmospheric attenuation at the exclusion of all other possible sources of noise in the case of a perfectly-reflecting target. As before, our goal is to provide a simplified characterization of the independent impact of a particular source of sensor performance degradation so that the impact on available entanglement-derived information can be more clearly understood. From this section forward we will mostly concentrate our discussion on the entanglement-enabled quantum radar and what we have called a “coherent” radar which offers photon-by-photon control without entanglement. As explained before, this is the the best possible sensor that does not exploit entanglement and is used purely to establish an upper bound on the performance of a classical radar.

Given these assumptions the snr for a single photon state that traverses a round-trip distance r is

$$snr = \frac{\kappa N_s}{N_b} = \frac{N_s}{N_b} e^{-\chi r} \quad (30)$$

where κ represents the losses due to atmospheric attenuation or target reflectivity. In this section we are interested in examining effects of the atmosphere, so we assume a perfectly reflective target and only consider losses due to atmospheric scattering and absorption. The parameter χ represents the assumed attenuation constant for the atmosphere within the

Visibility (m)	$\lambda = 1.25\text{cm}$	$\lambda = 3.2\text{cm}$	$\lambda = 10\text{cm}$
30	0.2878	0.0460	0.0046
90	0.0576	0.0092	0.0009
300	0.0104	0.0016	0.0002

TABLE I
IMPACT OF CLOUDS ON THE ATTENUATION COEFFICIENT χ (1/KM) FOR DIFFERENT RADAR WAVELENGTHS (ASSUMING AN AMBIENT TEMPERATURE IN THE VICINITY OF 0°C).

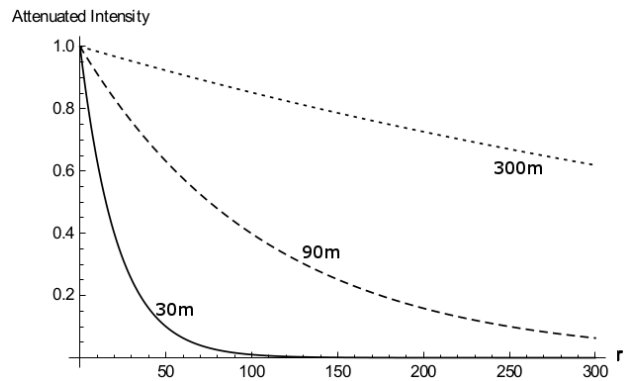


Fig. 7. $\lambda = 3.2\text{cm}$ radar attenuation as a function of range (in km) through clouds with visibility 30m (solid line), 90m (dashed line), and 300m (dotted line).

surveillance region and N_s is the average number of Gaussian-state signal photons. Notice that to better illustrate the impact of the atmospheric attenuation, we are assuming a perfectly reflective target. Based on the SPDC experiments [31], we will use the value $N_s \approx 10^{-4}$, thus leaving us to identify the practically relevant values of χ . Typical values for the case of clouds or fog for different wavelengths are given [68] in Table I.

Figure 7 shows attenuation as a function of distance for $\lambda = 3.2\text{cm}$, which is inside the radar X-band (2.5-3.75 cm; 8-12 GHz), through cloudy environments of different visibility ranges. The solid line represents the case of dense clouds with only 30m of visibility, i.e., a human would only be able to resolve objects out to a range of 30 meters. The dashed line corresponds to 90m visibility, and the dotted line corresponds to 300m visibility. As shown in Figure 7, $\chi \approx 0.046 \text{ km}^{-1}$ for radar wavelengths of $\lambda = 3.2\text{cm}$ in low visibility (30m) conditions.

Atmospheric attenuation strongly limits the effectiveness of radar, but this offers a potential advantage for low-brightness quantum sensing in stealth applications. More specifically, when there is a need for low-brightness target illumination the value of entanglement-derived information increases.

Using $\log_{10} \tilde{M} \approx 9.2668$ obtained earlier to maximize the quantum advantage for the signal-to-noise ratio per photon $snr = 10^{-9}$, we obtain a signal-to-noise ratio of $SNR \approx 2.7$ dB. Then, the respective upper bound detection error probabilities for the entanglement-based quantum sensor; coherent sensing with photon-by-photon control; and a classical radar obeying the Albersheim equation are respectively:

$$P_q \approx 0.08 \quad (31)$$

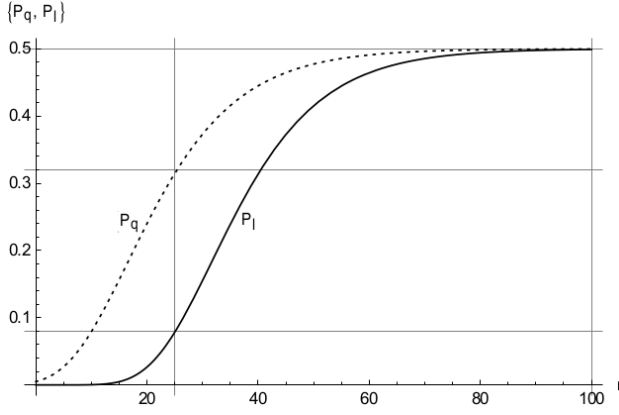


Fig. 8. Detection error probability bounds P_q (solid line) and P_l (dashed line) as a function of range r (in km) to the target.

$$P_l \approx 0.32$$

$$P_c \approx 0.43$$

Notice that in this specific case, entanglement information gives the quantum sensor a 4x improvement over lidar and 5.38x improvement over classical. However, as we discussed before, in general entanglement-based quantum radar offers a 6 dB advantage in the error-probability exponent over the optimal coherent receiver that does not use entanglement. And therefore, the maximum advantage offered by a quantum radar over any other sensor that does not use entanglement is approximately 6 dB. Calculating the maximum travel distance that satisfies our required average photon number of $N_s \approx 10^{-4}$, we find that attenuation from a 50km round trip reduces the number of photons received at the detector to 1.85×10^4 .

Figure 8 shows the detection error probability bounds P_q and P_l with \tilde{M} photons under low visibility conditions. The quantum advantage is clearly significant in a window around the 25km range-to-target distance but decreases rapidly beyond 60km and is negligible beyond a distance of 80km, at which both sensors become essentially uninformative. For a target at 100km only 0.01% of the transmitted photons return to the detector, and at 132km only 1 photon is expected to return.

The plots of Figure 8 suggest that the behaviors of P_q and P_l are nearly identical up to a horizontal shift, i.e., up to a difference in range-to-target distance. The reason can be seen by considering

$$P_q(r) = \frac{e^{-\tilde{M}N_s\kappa(2r)/N_b}}{2} \quad P_l(r) = \frac{e^{-\tilde{M}N_s\kappa(2r)/4N_b}}{2} \quad (32)$$

where $\kappa(2r)$ represents the total photon attenuation as a function of the entire traversal distance of returned photon states ($2r$). Thus

$$P_q(r) = P_l(r - z) \quad (33)$$

which is equivalent to

$$e^{-\tilde{M}N_s\kappa(2r)/N_b} = e^{-\tilde{M}N_s\kappa(2r-2z)/4N_b} \quad (34)$$

and consequently:

$$4\kappa(2r) = \kappa(2r - 2z) \implies e^{\chi 2z} = 4 \quad (35)$$

$$\implies z = \frac{\ln 4}{2\chi} \quad (36)$$

which corresponds to $z \approx 15$ km. In the case of the assumed attenuation coefficient, this says that if the classical sensor achieves a particular detection error probability for a target at distance r , the quantum sensor will achieve the same probability for a target at distance $(r + 15)$ km. Of course the specific value of the quantum range advantage is determined by the assumed attenuation coefficient, but it is theoretically nonzero for any detection error probability within the open admissibility interval between 0.0 and 0.5. In fact, this can be interpreted as a measure in units of distance of the information potentially available from entanglement in the source photons.

IX. QUANTUM STEALTH

Returning to considerations of stealth sensing, the goal is to achieve a practical detection capability while limiting an adversary's practical ability to detect our radiated sensing signals. Under our present set of assumptions, less than 1 of the \tilde{M} transmitted photon states will survive attenuation at a range of $R_e \approx 264$ km, so intuitively the effective SNR that an adversary detector must accommodate to identify our location is quite formidable. In fact, if the finite operation time of our sensor is less than the integration time necessary for the adversary to achieve a detection then for all practical purposes the sensing operation will be invisible to the adversary. This motivates a definition of *stealth* in terms of a threshold for detection by an adversary.

For example, we could choose a stealthiness threshold based on a detection error probability that is nearly 0.5 so that an adversary's level of confidence in a possible detection of our sensor will be comparable to that of a coin toss. As can be expected – and will be seen – the difficulty we face in satisfying such a threshold increases exponentially as it approaches the 0.5 limit of perfect stealth. To make the analysis concrete, we will arbitrarily choose 0.4 as the acceptable detection error probability we are willing to allow for the adversary. In a real-world application a meaningful utility function would likely be available, e.g., relating to the cost we would expect to incur if the adversary is able to confidently detect our sensor.

Stealth sensing has strong foundational connections to secure communication theory. For example, as is the case in establishing provable levels of security in cryptographic applications, worst-case assumptions must be assumed about the technological capabilities of the adversary. In our case this equates to assuming the adversary has perfect line-of-sight detectors for measuring all photon states. Under this assumption the *interception error probability* for an adversary sensor at distance r from a quantum entangled photon emitter platform is

$$\pi_q = \frac{e^{-\tilde{M}N_s e^{-\chi r}/(4N_b)}}{2} \quad (37)$$

which means that small π_q implies that the adversary's error in determining the location of our platform is small. Thus

in the limit of $\pi_q = 0$ the adversary can potentially determine the presence of the platform with complete confidence. Alternatively, in the limit of $\pi_q = 0.5$ the adversary cannot ascertain the presence of our platform with any confidence greater than a coin flip, i.e., we achieve perfect stealth. Of course this limit cannot actually be achieved in practice, so we will have to determine whether there exists some lesser value that satisfies the performance requirements of the overall application. In summary, we wish to identify the largest value less than $\pi_q = 0.5$ that we can confidently impose on the adversary.

To simplify our analysis, let us now consider a coherent sensor that has the exact same detection error probability as an entangled photon sensor. This can be done at the expense of a larger number of unentangled photon states. Indeed, let us recall that the difference between the detection error probabilities upper bounds for entanglement-based quantum radar and for non-entangled coherent sensing is a factor of 4 in the denominator of the exponent. Thus, if the coherent sensor uses four times the number of entangled photon states, then both systems have the same detection error probability. Then, the interception error probability for an adversarial sensor located at a distance r from the coherent system operating with $4\tilde{M}$ photons is given by:

$$\pi_l = \frac{e^{-\tilde{M}N_s e^{-\chi r}/N_b}}{2} \quad (38)$$

which differs by a factor of $1/4$ in the argument of the exponential because the coherent sensor emits $4x$ as many entangled photons as the number of unentangled photons produced by the coherent sensor.

To reiterate, we are comparing an entanglement-based quantum radar and a coherent sensor operating at the same detection error probability. For this to happen, the coherent sensor has to operate with 4 times more signal photons than the entanglement-based quantum radar. The detection error probability of an adversarial sensor is given by the expressions π_q and π_l . Clearly, because the coherent system uses more photons, it will be more likely to be detected by an adversary.

Indeed, assuming the adversary sensor is located at distance r from our sensor then the relative performance obtained using a quantum versus coherent sensor can be seen from the behavior of π_q (solid line) and π_l (dashed line) as shown in Figure 9. From this it can be verified that the stealth bound is satisfied by the quantum sensor up to a range of 96km while the lidar can do so only up to 66km. Thus the quantum sensor provides an additional 30km of stealth sensing range, while at ranges less than 66km both sensors satisfy the required level of stealth.

As should not be surprising from our previous examination of entangled-vs.-non-entangled detection error probabilities, the plots of π_q and π_l are the same up to a simple shift:

$$\pi_q(r) = \pi_l(r + z) \quad (39)$$

which is equivalent to

$$e^{-\tilde{M}N_s \kappa(r)/4N_b} = e^{-\tilde{M}N_s \kappa(r+z)/N_b} \quad (40)$$

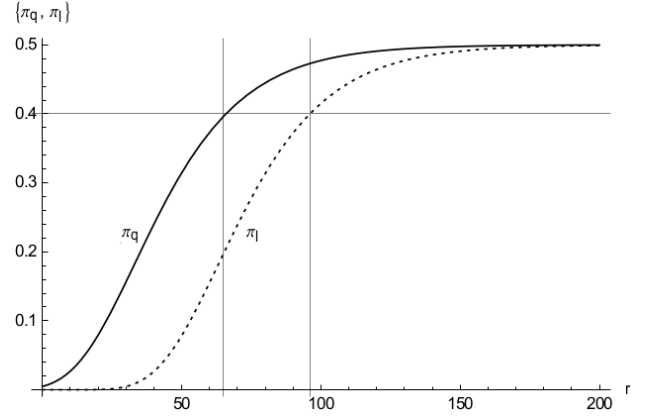


Fig. 9. An adversary sensor's interception error probability at a distance r (in km) from a quantum radar (π_q , solid line) and a lidar (π_l , dashed line).

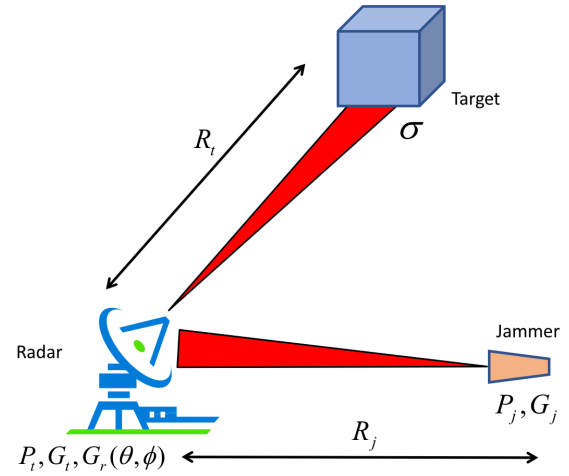


Fig. 10. Jamming as an active detection countermeasure.

and thus

$$\frac{1}{4} \kappa(r) = \kappa(r + z) \implies e^{-\chi z} = \frac{1}{4} \implies z = \frac{\ln 4}{\chi}, \quad (41)$$

which in our case represents a shift of $z \approx 30$ km. The conclusion to be drawn is that the analysis of an adversary's interception detection probability exactly mirrors that of our previous analysis of sensor detection error probability.

X. QUANTUM ROBUSTNESS TO JAMMING

Although slightly more complex to analyze, the quantum advantage seen thus far in the cases of detection and interception error probabilities extends also to robustness against active sensing countermeasures by an adversary, i.e., active jamming of our sensor [67], [68]. This involves adversarial transmission of noise photons toward our sensor in order to reduce the effective SNR available to our system. Figure 10 shows a concrete example of an adversary aircraft transmitting jamming noise toward a sensor to limit its ability to detect and/or track a target aircraft.

Jamming has been a major focus of classical radar research for over 70 years and is commonly examined using a simple mathematical expression referred to as the *jamming equation*

[29]. Following the general spirit of this paper, we use this simple jamming model to compare quantum and classical detection, but we acknowledge that in reality the behavior of jammers is much more complex. This equation relates a target that is characterized by its assumed radar cross section σ ; electromagnetic jamming waves with power P_j and gain G_j ; a transmitter that has power P_t and gain G_t ; and a radar receiver with gain G_r defined as a function of angular observation variables θ and ϕ .

The signal power after being reflected by the target is expressed by the following *radar equation* as:

$$P_r^{(t)} = \frac{P_t G_t G_r(\theta_t, \phi_t) \lambda^2 \sigma}{(4\pi)^3 R_t^4} \quad (42)$$

and a related equation can be derived that incorporates the effect of a jamming signal of power $P_r^{(j)}$:

$$P_r^{(j)} = \left(\frac{P_j G_j}{4\pi R_j^2} \right) \times \left(\frac{\lambda^2 G_r(\theta_j, \phi_j)}{4\pi} \right) \quad (43)$$

These two equations can then be used to define a *signal-to-jam ratio* (SJR):

$$\text{SJR} = \frac{P_r^{(t)}}{P_r^{(j)}} = \left(\frac{P_t G_t}{P_j G_j} \right) \times \left(\frac{R_j^2}{R_t^4} \right) \times \left(\frac{\sigma}{4\pi} \right) \times \left(\frac{G_r(\theta_t, \phi_t)}{G_r(\theta_j, \phi_j)} \right) \quad (44)$$

The distance at which $\text{SJR} \approx 1$, i.e., when the jamming system is effectively able to mask the target's return signal, is referred to as the *burnthrough range* [29]. In other words, within the context of this simple model, jamming by an adversary will be effective when $\text{SJR} < 1$ as the radar will not be able to separate the return signal of the target from the total noise entering the system. More generally, jamming becomes increasingly more effective as

$$R_j \approx R_t \implies \frac{R_j^2}{R_t^4} \ll 1 \quad (45)$$

while a radar looking in the direction of the target becomes increasingly more effective as

$$G_r(\theta_t, \phi_t) \gg G_r(\theta_j, \phi_j) \implies \frac{G_r(\theta_t, \phi_t)}{G_r(\theta_j, \phi_j)} \gg 1. \quad (46)$$

From this we can analyze the effectiveness of a quantum radar compared to a non-entangled coherent system with the SJR expressed similarly as

$$\text{SJR}_q = \frac{\tilde{M} P_r^{(t)}}{P_r^{(j)}} = \frac{\tilde{M} N_s e^{-\chi 2 R_t}}{N_j e^{-\chi R_j}} = \frac{\tilde{M} N_s}{N_j} e^{-\chi(2R_t - R_j)} \quad (47)$$

where N_j is the number of noise photons injected into the sensor by the jammer. If the jamming signal emanates from target itself, i.e., $R_t = R_j$, then:

$$\text{SJR}_q = \frac{\tilde{M} N_s}{N_j} e^{-\chi R_t}. \quad (48)$$

In this case the burnthrough range condition simplifies to

$$\text{SJR}_q = \frac{\tilde{M} N_s}{N_j} e^{-\chi R_t} < 1 \implies \tilde{M} N_s e^{-\chi R_t} < N_j \quad (49)$$

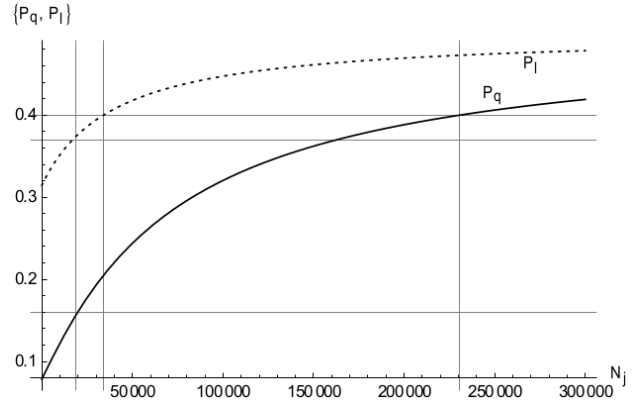


Fig. 11. Detection error probabilities P_q (solid line) and P_l (dashed line) as a function of the number N_j of jamming photons.

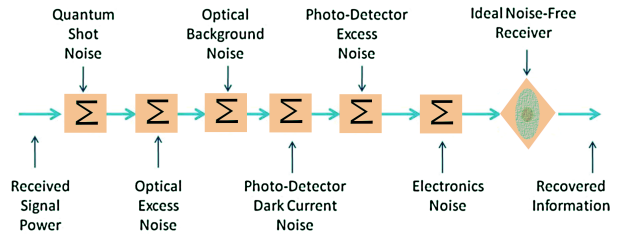


Fig. 12. Additive noise sources affecting the photodetector [61].

and the resulting signal-to-noise ratio SNR available to the sensor becomes

$$\text{SNR} = \frac{\tilde{M} N_s e^{-\chi R_t}}{N_b + N_j e^{-\chi R_j}}. \quad (50)$$

In the case of a target at 25km (under the same as assumptions as in our previous examples) the burnthrough range condition is $N_j > 18532$. Figure 11 shows the effect of jamming on the detection error probabilities P_q and P_l . In the clear case of no jamming, i.e., $N_j = 0$, it can be seen that $P_q \approx 0.08$ and $P_l \approx 0.32$, as we previously determined. It can also be seen that the detection error probability approaches the noninformative limit of 0.5 as N_j increases.

The first vertical grid line in Figure 11 corresponds to $P_q \approx 0.16$ and $P_l \approx 0.37$ at which the burnthrough range condition is $N_j = 18532$. Continuing with our prior chosen threshold of 0.4 on the adversary's allowed detection error probability, we see from the second vertical grid line that the adversary would require $N_j \approx 33990$ noise photons to effectively jam the classical sensor but a factor of 7 more noise photons ($N_j \approx 230705$) to jam the quantum sensor.

XI. NOISE IN QUANTUM RADAR

We consider six major sources of noise in the scenarios of interest here: quantum shot noise, optical excess noise, photodetector dark current noise, photodetector excess noise, and electronics noise [1], [9], [11], [24], [61], [63]. These are assumed to be additive as depicted in Figure 12.

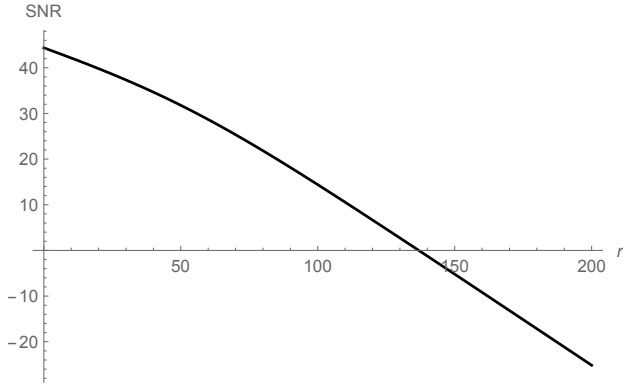


Fig. 13. SNR (dB) as a function of target distance r (in km).

As a concrete example, consider the signal-to-noise ratio in the case of $N = 10^5$ effective signal photon states (corresponding to $M = 10^9$ emitted signal states of small photon density $N_s = 10^{-4}$), noise photon density $N_b = 10^4$, signal photon wavelength $\lambda = 3.2\text{cm}$, effective noise bandwidth $\Delta\nu = 1\text{Hz}$, atmospheric attenuation $\chi = 0.046\text{km}^{-1}$, target reflectivity $\eta = 0.6$, and dark count rate $R = 1\text{Hz}$. As will be discussed in the following section, these are realistic values for a scenario involving observations from a low-brightness quantum radar within a low-visibility volume of the atmosphere. In the case of a target at distance r the SNR is determined by the photon round-trip distance of $2r$ and it is shown in Figure 13. As should be expected, the SNR decreases exponentially with increasing target distance as a result of atmospheric attenuation and scattering.

The relative impact of the three most important noise sources can be examined in terms of the average number of photons contributed by each:

$$\begin{aligned} N_\sigma &\equiv \frac{2 \Delta\nu}{\eta} & (51) \\ N_\beta &\equiv \frac{2 \Delta\nu}{\eta} \frac{N_b}{N e^{-\chi r}} \\ N_{dc} &\equiv \frac{2R}{\eta^2 N e^{-\chi r}} \end{aligned}$$

It can be expected that the number of photons lost will increase exponentially with target distance and thus the SNR will decrease commensurately. At very large distances the sensor will primarily register dark counts or will detect photons based on the thermal background because virtually all signal photons will be lost. This means that the surveillance volume must be determined based on a chosen SNR threshold. Figure 14 reveals that solar background radiation dominates other sources in the regime of practical detection capability, which should not be surprising.

Clearly there are myriad important practical factors that will significantly impact any performance comparison of future real-world implementations of a quantum radar to its classical alternatives beyond what could be incorporated into our analysis. However, we can examine some of our simplifying assumptions, e.g., ignoring of the contribution dark counts and shot noise in our assumed number of noise photons N_b .

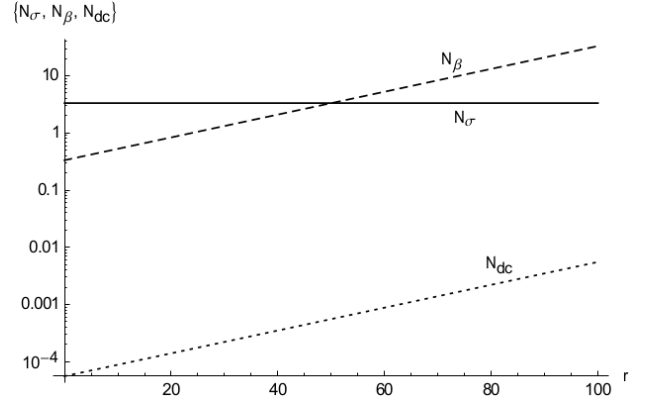


Fig. 14. Values of N_σ (solid line), N_β (dashed line) and N_{dc} (dotted line) as a function of target distance r (in km).

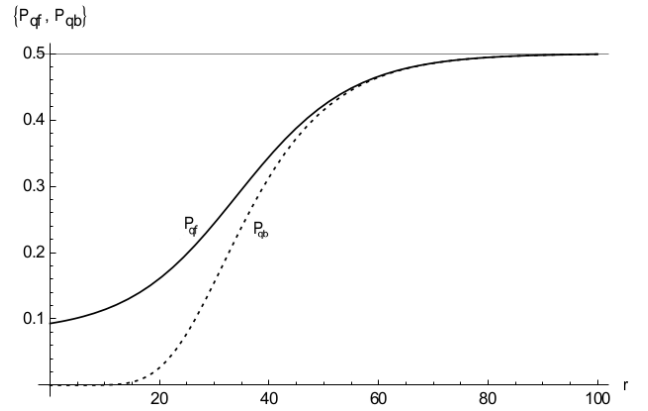


Fig. 15. Detection error probability bounds assuming a more complete noise model P_{qf} (solid line) versus a pure solar-produced background noise P_{qb} (dashed line) as a function of target distance r (in km).

Because the dark count contribution can be expected to be very small in our example scenarios (target ranges less than 100km) we can effectively model the joint contribution of dark count and shot noise as:

$$N_b \longrightarrow N_b + N_s M e^{-\chi r}. \quad (52)$$

Figure 15 shows the detection error probability bounds using this more complete noise model P_{qf} compared to pure solar background noise P_{qb} as a function of target distance r (in km). It can be observed that the higher-fidelity model implies significantly worse detection error probabilities in the regime of high SNR when the target range r is small because shot noise becomes increasingly dominant. The impact of the higher-fidelity noise model (i.e., with $N_b \approx N_b + N_s M e^{-\chi r}$) on the relative advantage in detection error probability of quantum (P_{qf}) over classical (P_{lf}) is shown in Figure 16. It can be seen that the breakthrough threshold of 0.4 is reduced to 47km for quantum and 26 km for classical, but the quantum advantage in range *improves* from 15 km to 21 km compared to our simplified background-only model.

XII. THE CHALLENGES AHEAD

In summary, our analysis – *despite its many assumptions and limitations* – presents a compelling case for undertaking

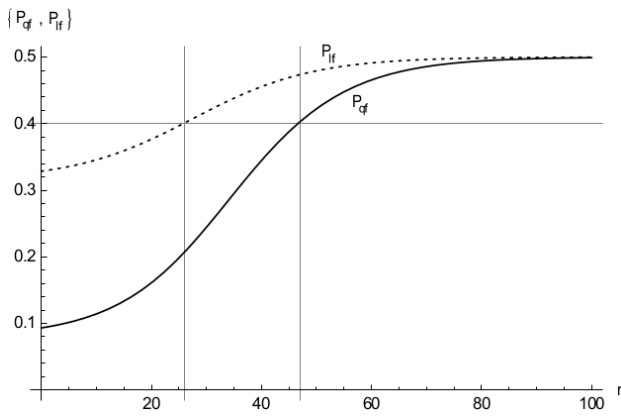


Fig. 16. Detection error probability bounds using the full noise model for the entanglement-based P_{qf} (solid line) and non-entangled P_{tf} (dashed line) sensor with respect to the distance r (in km).

the substantial scientific and engineering efforts necessary to determine the extent to which the theoretical quantum advantage can be realized in real-world systems. These include:

- Entangled Microwave Photon Generation:** By far the most critical challenge is the fast and efficient generation of entangled photons in microwave frequencies. As we have shown based on purely theoretical considerations, a signal package with more than 10^9 entangled photons is required to determine the presence of a target 25km away with detection probability of about 0.8 in low visibility conditions. If the target is in motion, which is the most realistic scenario, the entire signal package needs to be generated, emitted, and processed in a short period of time so that the process can be repeated multiple times. This means that it will likely be necessary to generate more than 109 entangled photons *per millisecond* if the target is in motion at a range of around 25km (the exact amount will of course depend on many factors such as the target speed, the target cross section, and the quantum radar wavelength). While the use of nonlinear crystals to generate entangled optical photons is very well understood from a theoretical and experimental point of view, much less is known about how to do so in the microwave regime. Potentially viable proposals have been made for the use of quantum dots; resonant QED cavities; and down conversion from optical frequencies; but presently the generation of even a small number of entangled microwave photons remains a huge scientific and technological challenge [44]. In addition, an ideal source of entanglement for sensing applications would produce entangled pairs on demand; that is, with near 100% certainty the source produces exactly 1 entangled pair at the push of a button; however, such sources are in their infancy and not commercially available.
- Distinguishable Optical Modes:** A related challenge is the number of distinguishable optical modes available on each millisecond-long signal package [19], [35]. Because quantum radar exploits the photon-level correlations between entangled signal and idler photons, it is necessary to have these photons in distinguishable optical modes

so they can be properly sorted out by the system. In the case of X-band photons, for instance, with a 40% fractional bandwidth and a 600 MHz frequency bandwidth, a millisecond signal package can only have about 4,000 distinguishable optical modes. This is substantially below the required 10^9 required for optimal quantum sensing at 25km and could lead to extremely large integration times [19]. Even though there have been some proposals to address this problem, including the design of virtual modes in a parallel architecture and using multiple-input multiple-output channels using beam-splitters, considerable research is still required to overcome this obstacle [25], [33], [35].

- Quantum Memories:** As described in Figure 1, the idler photon needs to be stored in a robust and reliable quantum memory. This memory has to faithfully hold the quantum state of the idler photon for a period of time determined by the time of travel of the signal photon. In addition, the process of comparing the idler and received signal photons requires the construction of non-trivial quantum operators that act on both photon states. These operations are accomplished using quantum gates similar to those required for a quantum computer. Fortunately, current research on fault-tolerant quantum computation is making progress toward near-term practical and dependable long decoherence-time quantum memories and fault-tolerant gates [21]. In addition, some proposals such as “quantum noise radar” may circumvent the need of a quantum memory [64].
- Single Photon Detectors:** Equally fundamental for the design of a fully functional quantum radar is the development of improved single photon detectors with very high detection efficiencies yet very small dark currents and excess noise. As with the case of quantum memories, such devices are receiving a significant level of research focus because of their need in other quantum technologies such as secure quantum key distribution [44].
- Signal Processing:** The signal photon is expected to traverse an attenuating environment, so at near 0 dB SNR most of the signal photons will be scattered or absorbed by air molecules and will never reach the detector. Furthermore, some of these photons may be received out of synch with the idler photons stored in the quantum memory. Consequently there is a strong need to develop robust signal processing techniques able to extract as much useful target information as possible from the few signal photons that are received by the detector. This requires identification of the specific encodings of the signal photons that provide the best resilience to corruption under the environmental conditions of relevance to the application of interest [10]. In addition, we need to develop robust techniques to optimize the integration time of the information from all the returning signal photons.
- Detection and Ranging Protocols:** To date, no efficient quantum ranging protocol has been developed. While quantum illumination offers very interesting advantages, it is only a detection protocol, i.e., is only concerned with determining if a target is present or not at a specific

point of space). Ranging protocols to actually estimate the distance to the target have proved to be very challenging to design. The likely reason is that most entanglement-based standoff quantum sensing devices appear to require single-photon control, where each signal photon and its entangled idler counterpart need to be identified to extract target information from the entanglement correlations. It is clearly not feasible to illuminate and probe a large region of space using these techniques. However, intriguing proposals such as “progressive quantum scanning” (exploiting some existing information about the target) and “quantum noise radar” (exploiting the entanglement represented by the statistical properties of a group of photons) appear to be able to circumvent this problem to some degree [43], [64]. Nonetheless, further research in this area is required for the design of quantum detection and ranging devices when no other target information is available.

- **Quantum Hardware:** In general, most detection and ranging protocols will require sophisticated quantum hardware to perform operations and measurements on the photon states. For example, basic quantum illumination requires a very specific type of joint measurement [22]. Even though quantum illumination has been demonstrated experimentally, this was done using a suboptimal receiver that only achieved a 3 dB advantage (instead of the predicted 6 dB) [18]. Short of a general-purpose quantum computer, even the most simple design of an optimal quantum illumination receiver requires sophisticated quantum operations on the pair of entangled photons [74]. Therefore, it is necessary to develop robust quantum hardware to implement any sophisticated quantum detection and ranging system. Fortunately, quantum hardware is currently being developed within the context of quantum computation [59].
- **Target Interaction:** Besides their interaction with the attenuating environment, some of the signal photons may also interact with the target before being reflected back to the detector. In general, the target may have a sophisticated geometry and may be moving in a non-trivial manner [69]. Also, the target may be composed of layered materials with specific electromagnetic properties. Thus, we need to improve our understanding of the details of these kinds of photon-target interactions so they can be modeled with higher fidelity, e.g., for better quantum radar cross section models that provide more than simply “target in/outside range” classifications [4]–[8], [37], [49]. For example, it is important to determine how Doppler or other signatures in quantum radar can be used to determine the presence of moving parts in the target (e.g., fan or helicopter blades); to reduce the effects of clutter (e.g., due to hail or radar countermeasures); or for target discrimination (e.g., to determine if there is a single target or many clustered targets). Even though radar cross sections is an important issue for classical radar systems, quantum interactions and measurement protocols could lead to novel effects not seen in the classical domain.

- **Quantum Attenuation Models:** As quantum radar is a standoff sensing technique, the signal photons are expected to traverse a noisy and attenuating environment [40], [44]. That is, signal photons will be lost to absorption and scattering produced by molecules in the environment. Currently the classical interaction between signal photons and the environment is modeled with a macroscopic bulk material approximation [44]. However, the transition to quantum-based sensing modalities offers an opportunity to develop and exploit higher-fidelity attenuation models using the fully quantized Maxwell’s equations in presence of material media [56], [57]. Such models could create or significantly improve the quantum advantage over classical in some scenarios and therefore represents a potentially high-impact research topic. Once again, even though attenuation is an important issue for classical radar systems, certain quantum interactions with the environment could lead to novel effects not seen in the classical domain.
- **Sensor System Design:** Finally, it is important to note that quantum radar cannot be expected to replace classical radar and other traditional sensing methods. In any realistic context it will be necessary to design a mixed system of quantum and classical sensor components that best leverages their relative advantages with respect to the scenario of interest [38], [39]. In some sense this may seem less daunting than the previous challenges because the characteristics of quantum sensing technologies can in theory be incorporated into the component spreadsheet of the system design optimization process just like any other classical component. However, it is likely that the distinctly non-classical performance characteristics of quantum technologies will radically change the nature and complexity of the problem [38]. In fact, it may prove necessary to apply quantum optimization technologies to obtain practical solutions in a reasonable amount of time.
- **System Information Exploitation:** The fact is that what constitutes the “best” system for a given application depends critically on the filtering and tracking algorithms that will process the information provided by the system [38], [39]. If this information is partially quantum in nature then traditional estimation and filtering methods will have to be generalized accordingly to optimally exploit that information [38]. Clearly, improvements to these methods will affect the relative performances of different system configurations, and therefore will impact the optimization problem to be solved by the sensor system design process, i.e., the problems of sensor system design and system information exploitation are not really independent.

XIII. CONCLUSIONS

This paper provides a simple back-of-the-envelope and implementation-agnostic analysis to glimpse the kinds of expected improvement that a quantum detection and ranging system could provide for applications of interest. Such analyses of course cannot lead to definitive conclusions, but we believe

they provide evidence that in some contexts quantum radar can be expected to offer realizable practical advantages over classical alternatives.

As quantum entanglement offers an advantage on the small signal-to-noise regime (approximately from -15 to 20 dB), the applications of quantum radar may be limited to those that require the detection of targets using the minimum amount of energy that is possible. For example, stealth sensing for military applications or for medical imaging where it is desirable to keep radiation levels to a minimum. On the other hand, if no low energy sensing constraints exist, then classical radar will be preferable to quantum radar. Indeed, in the large signal-to-noise regime, the classical radar will operate with a similar detection probability as quantum radar, but without the enormous technological complexities involved with quantum hardware.

Of course, as we already mentioned, there are many scientific and engineering challenges that need to be addressed before we can assert the true advantage of quantum radar systems. Based on our previous discussion, we can now enumerate what we believe are the most important conclusions to be drawn from our examination of quantum detection and ranging:

- 1) Quantum entanglement represents a new and radically different source of information that theoretically can permit a quantum radar to significantly outperform its classical counterparts in multiple ways.
- 2) Analyses that are roughly analogous to back-of-the-envelope calculations provide a glimpse of the kinds of improvement that a quantum radar can provide in practical applications of interest.
- 3) Many practical engineering obstacles remain to be solved before the full potential of quantum radar can be realized.
- 4) All things considered, a strong case can be made that quantum radar research represents a “high risk” / “high payoff” endeavor that justifies further scientific and engineering consideration, investigation, analysis, and discussion.

REFERENCES

- [1] S.B. Alexander, *Optical Communication Receiver Design*, SPIE Press, 1997.
- [2] S. Barzanjeh, et al., “Microwave Quantum Illumination”, *Phys. Rev. Lett.*, 114, 080503, 2015.
- [3] S. Barzanjeh, et al., “Experimental Microwave Quantum Illumination”, arXiv:1908.03058 [quant-ph], 8 Aug. 2019.
- [4] MJ Brandsema, RM Narayanan, M Lanzagorta, “The effect of polarization on the quantum radar cross section response”, *IEEE Journal of Quantum Electronics*, vol. 53, no. 2, pp. 1-9, 2017.
- [5] MJ Brandsema, RM Narayanan, M Lanzagorta, “Cross section equivalence between photons and non-relativistic massive particles for targets with complex geometries”, *Progress in Electromagnetics Research*, Vol. 54, 37-46, 2017.
- [6] MJ Brandsema, RM Narayanan, M Lanzagorta, “Theoretical and computational analysis of the quantum radar cross section for simple geometrical targets”, *Quantum Information Processing*, 16:32, 2017.
- [7] M.J. Brandsema, RM. Narayanan, M. Lanzagorta, “Electric and magnetic target polarization in quantum radar”, *Proceedings of SPIE* Vol. 10188 (101880C), 2017.
- [8] M.J. Brandsema, R.M. Narayanan, M. Lanzagorta, “Analytical formulation of the quantum electromagnetic cross section”, *Proceedings of SPIE* Vol. 9829 (98291H), 2016.
- [9] M.J. Buckingham, *Noise in Electronic Devices and Systems*, Ellis Horwood Publishers, 1983.
- [10] T. Crowder and M. Lanzagorta, “Detection and Communication with Entanglement,” *IEEE Conference on Antenna Measurements & Applications (CAMA)*, Vasteras, Sweden, pp. 1-4, 2018.
- [11] E.L. Dereniak and D.G. Crowe, *Optical Radiation Detectors*, Wiley, 1984.
- [12] J.P. Dowling, “Quantum optical metrology - the lowdown on high-NOON states”, *Contemporary Physics*, Vol. 49, No. 2, 2008.
- [13] C. Emary, et al. “Emission of Polarized-Entangled Microwave Photons from a Pair of Quantum Dots”, *Phys. Rev. Lett.* 95, **127401**, 2005.
- [14] D.G. England, “Quantum-enhanced standoff detection using correlated photon pairs”, *Phys. Rev. A* 99, 023828, 2019.
- [15] V. Giovannetti, S. Lloyd, and L. Maccone, “Quantum Enhanced Positioning and Clock Synchronization”, *Nature* 412, 417, 2001.
- [16] V. Giovannetti, S. Lloyd, and L. Maccone, “Quantum-Enhanced Measurements: Beating the Standard Quantum Limit”, *Science*, 306, 2004.
- [17] V. Giovannetti, S. Lloyd, and L. Maccone, “Quantum Metrology”, *Phys. Rev. Lett.*, 96, 010401, 2006.
- [18] S. Guha and B. Erkmen, “Gaussian-state quantum-illumination receivers for target detection”, *Phys. Rev. A*, Vol. 80, 052310, 2009.
- [19] N. Hardy, B. Dixon, J. Shapiro, and S. Hamilton, “Quantum Illumination Radar Feasibility”, Slides presented to the *Emerging Technology Analytic Panel (ETAP)*, 11 December 2018.
- [20] C.W. Helstrom, *Quantum Detection and Estimation Theory*, Academic Press, (1976)
- [21] K. Heshami, et al., “Quantum memories: emerging applications and recent advances”, *Journal of Modern Optics*, 63:20, 2005-2028, 2016.
- [22] S. Hui-Tan, B.I. Erkmen, V. Giovannetti, S. Guha, S. Lloyd, L. Maccone, S. Pirandola, and J.H. Shapiro, “Quantum Illumination with Gaussian States”, *Phys. Rev. Lett.*, 101 (253601), 2008.
- [23] S.D. Huver, C.F. Wildfeuer, and J.P. Dowling, “Entangled Fock states for robust quantum optical metrology, imaging, and sensing”, *Phys. Rev. A*, 78, 063828, 2008.
- [24] G. Jacobsen, *Noise in Digital Optical Transmission Systems*, Artech House, 1994.
- [25] R. Jantti, R. Di Candia, R. Duan and K. Ruttik, “Multiantenna Quantum Backscatter Communications,” *IEEE Globecom Workshops (GC Wkshps)*, Singapore, pp. 1-6, 2017.
- [26] Jin, R.-B. et al. Highly efficient entanglement swapping and teleportation at telecom wavelength, *Sci. Rep.* 5, 9333 (2015).
- [27] Jin, R.-B., et al., “Pulsed Sagnac polarization-entangled photon source with a PPKTP crystal at telecom wavelength”, *Opt. Express* 22, 11498-11507 (2014).
- [28] Jin, R.-B., et al., “Efficient detection of an ultra-bright single-photon source using superconducting nanowire single-photon detectors”, *Opt. Commun.* 336, 47-54 (2015).
- [29] D.C. Jenn, *Radar and Laser Cross Section Engineering*, Second Edition, AIAA Press, 2005.
- [30] K.T. Kapale, L.D. Didomenico, H. Lee, P. Kok, and J.P. Dowling, “Quantum Interferometric Sensors”, *Proc. SPIE 6603, Noise and Fluctuations in Photonics, Quantum Optics, and Communications*, 660316 (8 June 2007); doi: 10.1117/12.724317.
- [31] P. Kok and B.W. Lovett, *Introduction to Optical Quantum Information Processing*, Cambridge University Press, 2010.
- [32] M. Lanzagorta and J. Uhlmann, “Assessing Feasibility of Secure Quantum Communications Involving Underwater Assets,” *IEEE Journal of Oceanographic Engineering*, 2019.
- [33] M. Lanzagorta and J. Uhlmann, “Virtual Modes for Quantum Illumination”, *IEEE Conference on Antennas & Applications (CAMA)*, Vasteras, Sweden, 2018.
- [34] M. Lanzagorta and J. Uhlmann, “Theoretical Foundations for Design of a Quantum Wigner Interferometer”, *IEEE Journal of Quantum Electronics*, Vol. 55, No. 1, 2019.
- [35] M. Lanzagorta, J. Uhlmann, T. Le, O. Jitrik, S.E. Venegas-Andraca, “Improving quantum sensing efficiency with virtual modes,” *Proceedings of SPIE*, Vol. 9829 (98291D), 2016.
- [36] M. Lanzagorta, O. Jitrik, J. Uhlmann, S.E. Venegas-Andraca, “Clutter attenuation using the Doppler effect in standoff electromagnetic quantum sensing,” *Proceedings of SPIE*, Vol. 9829 (98291E), 2016.
- [37] M. Lanzagorta, “Amplification of radar and lidar signatures using quantum sensors,” *Proceedings of SPIE* Vol. 8734 (87340C), 2013.
- [38] M. Lanzagorta, O. Jitrik, J. Uhlmann, S.E. Venegas-Andraca, “Data fusion in entangled networks of quantum sensors”, *Proceedings of SPIE*, Vol. 10200 (10200M), 2017.
- [39] M. Lanzagorta, “Quantum Processing for Sensor Networks”, *Software Guru #58* (in spanish), 2019.

- [40] M. Lanzagorta, "Low Brightness Quantum Radar," *Proc. of the SPIE Radar Sensor Technology Conference*, Vol. 9461, 946113, 2015.
- [41] M. Lanzagorta, O. Jitrik, J. Uhlmann, S.E. Venegas-Andraca, "The Lemur Conjecture", *Proceedings of SPIE* Vol. 10188 (101880D), 2017.
- [42] M. Lanzagorta, O. Jitrik, J. Uhlmann, S.E. Venegas-Andraca, "Quantum seismography", *Proceedings of SPIE*, Vol. 9829 (98291G), 2016.
- [43] M. Lanzagorta, "Quantum imaging for underwater arctic navigation", *Proceedings of SPIE* Vol. 10188 (101880G), 2017.
- [44] M. Lanzagorta, *Quantum Radar*, Morgan & Claypool, 2012.
- [45] M. Lanzagorta, *Quantum Information in Gravitational Fields*, Institute of Physics - IOP Publishing, 2014.
- [46] M. Lanzagorta, *Nanomagnet-based magnetic anomaly detector*, US Patent No. 8,054070 B1, Nov. 8, (2011)
- [47] M. Lanzagorta, J. Uhlmann and S.E. Venegas-Andraca, "Quantum sensing in the maritime environment," *OCEANS 2015 - MTS/IEEE Washington*, Washington, DC, 2015, pp. 1-9.
- [48] M. Lanzagorta and J. Uhlmann, "Quantum imaging in the maritime environment," *OCEANS 2017 - Anchorage*, Anchorage, AK, pp. 1-10, 2017.
- [49] M. Lanzagorta, O. Jitrik, J. Uhlmann, S.E. Venegas-Andraca, "Clutter attenuation using the Doppler effect in standoff electromagnetic quantum sensing", *Proceedings of SPIE* Vol. 9829, 98291E (2016).
- [50] M. Lanzagorta, O. Jitrik, J. Uhlmann, S.E. Venegas-Andraca, "Quantum synthetic aperture radar", *Proceedings of SPIE* Vol. 10188, 101880F (2017)
- [51] S.K. Liao, et.al., "Satellite-to-ground quantum key distribution", *Nature*, Vol. 549, 43-47, 2017.
- [52] S. Lloyd, "Enhanced Sensitivity of Photodetection via Quantum Illumination", *Science*, Vol. 321, No. 5895, 2008.
- [53] P. van Loocke, "Entanglement Theory with Continuous Variables", in D.Bruß and G.Leuch, *Lectures on Quantum Information*, Wiley-VCH, (2007)
- [54] E.D. Lopaeva, et.al., "Experimental Realization of Quantum Illumination", *Phys. Rev. Lett.*, 110, 153603, 2013.
- [55] D. Luong, et.al., "Receiver Operating Characteristics for a Prototype Quantum Two-Mode Squeezing Radar", arXiv:1903.00101v1 [quant-ph], 2019.
- [56] K. Martin, T. Crowder, J. Feng, "Quantum error reduction without coding," *Proc. SPIE 9461, Radar Sensor Technology XIX; and Active and Passive Signatures VI*, 946114 (21 May 2015).
- [57] K. Martin, "The scope of a quantum channel." *Proceedings of Symposia in Applied Mathematics*. Vol. 71. 2012.
- [58] J.M. McGuirk et al, "Sensitive absolute-gravity gradiometry using atom interferometry", *Phys. Rev. A* 65 033608, 2002.
- [59] National Academies of Sciences, Engineering, and Medicine. *Quantum Computing: Progress and Prospects*, Washington, DC: The National Academies Press, 2019.
- [60] M.A. Nielsen and I.L. Chuang, *Quantum Computation and Quantum Information*, Cambridge University Press, (2000).
- [61] G.R. Osche, *Optical Detection Theory*, Wiley-Interscience, 2002.
- [62] G. Romero, et.al., "Microwave Photon Detector in Circuit QED", *Phys. Rev. Lett.*, **102**, 173602, 2009.
- [63] B.A.E. Saleh and M.C. Teich, *Photonics*, Second Edition, Wiley-Interscience, 2007.
- [64] C.W. Sandbo Change, et.al., "Quantum-Enhanced Noise Radar", *Appl. Phys. Lett.* 114, 112601 (2019).
- [65] M. Sanz, K.G. Fedorov, F. Deppe and E. Solano, "Challenges in Open-air Microwave Quantum Communication and Sensing," *2018 IEEE Conference on Antenna Measurements & Applications (CAMA)*, Vasteras, Sweden, pp. 1-4, 2018.
- [66] R. Simon, "Peres-Horodecki Separability Criterion for Continuous Variable Systems", *Phys. Rev. Lett.* 84, 2726, (2000)
- [67] M.L. Skolnik, *Introduction to Radar Systems*, Third Edition, McGraw Hill, 2001.
- [68] M.L. Skolnik, *Radar Handbook*, Third Edition, McGraw Hill, 2008.
- [69] J.E. Swan, M. Lanzagorta, D. Maxwell, E. Kuo, J. Uhlmann, W. Anderson, H.-J. Shyu, W. Smith, "A Computational Steering System for Studying Microwave Interactions with Missile Bodies", *IEEE Visualization 2000 (Proceedings of the IEEE Conference on Visualization '00)*, pp. 441-444, 2000.
- [70] J. Uhlmann and M. Lanzagorta, "Space-based quantum sensing for detection of small targets," *Proceedings of SPIE DSS, Radar Sensor Technology XIX*, April 2015.
- [71] J. Uhlmann, M. Lanzagorta and S.E. Venegas-Andraca, "Quantum communications in the maritime environment," *OCEANS 2015 - MTS/IEEE Washington*, Washington, DC, pp. 1-10, 2015.
- [72] S.E. Venegas-Andraca, M. Lanzagorta and J. Uhlmann, "Maritime applications of quantum computation," *OCEANS 2015 - MTS/IEEE Washington*, Washington, DC, pp. 1-8, 2015.
- [73] M.J. Woolley, C. Lang, C. Eichler, A. Wallraff and A. Blais, "Signatures of Hon-Ou-Mandel interference at microwave frequencies" *New Journal of Physics*, Volume 15, October 2013.
- [74] Zhuang et. al., "Optimum mixed state discrimination for noisy entanglement-enhanced sensing," *Phys. Rev. Lett.*, Vol 118, 040801, 2017.